



# IJIRSET

International Journal of Innovative Research in  
**SCIENCE | ENGINEERING | TECHNOLOGY**

e-ISSN: 2319-8753 | p-ISSN: 2320-6710



# INTERNATIONAL JOURNAL OF INNOVATIVE RESEARCH

IN SCIENCE | ENGINEERING | TECHNOLOGY

Volume 10, Issue 7, July 2021

**ISSN** INTERNATIONAL  
STANDARD  
SERIAL  
NUMBER  
INDIA

Impact Factor: 7.569



9940 572 462



6381 907 438



ijirset@gmail.com



www.ijirset.com



# PV-Charged Bidirectional EV Charger Compatible with Chademo and COMBO

Vandana G. Pawar<sup>1</sup>, Prof A. P. Kinge<sup>2</sup>, Prof S. G. Shete<sup>3</sup>

P.G. Student, Department of Electrical Engineering, TSSM's BSCOER, Pune, India<sup>1</sup>

Associate Professor, Department of Electrical Engineering, TSSM's BSCOER, Pune, India<sup>2</sup>

Assistant Professor, Department of Electrical Engineering, TSSM's BSCOER, Pune, India<sup>3</sup>

**ABSTRACT:** Electric vehicles (EVs) are considered to be the means of transportation of the future. They are more efficient and they don't have as many emissions compared to fossil fuel-powered vehicles. However, electric vehicles are currently charged from the grid. Its fuel structure is mainly based on fossil fuels. To make electric vehicles sustainable, charging them from a sustainable source of electricity is essential. Therefore, charging electric vehicles from photovoltaic (PV) panels is a suggestion for the future. At the same time, photovoltaic power generation has the characteristics of daily and seasonal changes. This requires a grid connection to ensure a reliable power source for charging electric vehicles. Office buildings, factories and other workplaces like industrial areas are ideal places to facilitate the charging of solar-powered electric vehicles and can be installed on the roofs of buildings and parking lots. With photovoltaic (PV) panels there are several advantages to charging electric vehicles. Since photovoltaics generate charging power locally, they reduce the grid's demand for electric vehicle charging power. EV batteries can be used as photovoltaic energy storage to reduce the negative impact of large-scale photovoltaic grid connections in the distribution network. Electric vehicles are parked for a long time in the workplace, and the energy consumption for charging is low, allowing Vehicle-to-Grid (V2G) technology in which electric vehicles act as controllable generators.

## I. INTRODUCTION

### A. Review

To charge EV from PV, the separate converter of EV and PV connected to the AC grid can be used. Alternatively, a single integrated converter connected to the EV, PV and the grid can be used. Several studies have proposed a three-port power converter for charging electric vehicles from PV. Direct DC charging for electric vehicles in the PV of the interconnected ZVTPWM buck converter is entered on the 210 V DC bus. A closed-circuit control was developed and a 2.4kW prototype was built to provide EV charging but not V2G. In the DC, the nanowire is used to charge photovoltaic electric vehicles, fuel cells and AC grids and 1.5 kW DC V DC full-bridge LLC resonant converters. The basic components of the system are used. A three-port 3.3 kW bidirectional 380 V DC link converter integrates electric, photovoltaic and single-phase AC power grids. The efficiency of the built-in converter has been increased by 7. Compared with separate converters for EV and PV, which is up to 15%. Two DC/DC converters for charging electric vehicles PV on the 48V backup battery in the 3.3kW system have no two-way power flow and are connected to the grid or isolated with the EV. A solar charging system for single-phase V2G V V2H scooters was developed. Functionally, it uses 2x12V low-voltage batteries, buck and boost converters for DCDC power conversion and a Hbridge for inverter operation. In previous studies, these designs were not suitable for high power (> 5 kW) three-phase applications. Consider electric vehicle charging standards in terms of charging current ripple, EMI, and V insulation. Similarly, after reviewing various EVPV topologies, the conclusion drawn is that most designs ignore the EV isolation requirements. High-frequency ALink based on multi-winding transformers is used to integrate EV, battery Storage and renewable energy. Although the topology provides the benefit of isolation between all ports and is suitable for high power, it is not suitable for EVPV applications for two reasons. European regulations have stipulated that photovoltaic energy and the grid need to be isolated. Secondly, PV and EV are essentially CC, so a link will cause unnecessary conversion steps. A 10 kW non-isolated bidirectional converter was proposed for charging EV from PV. Use of 575 V DC bus, integration and closed-loop control of EV, PV, and network are designed to reduce PV intermittently. Symmetrically, an isolated 5kW Zsource converter is used to charge electric vehicles from PV. Performance comparison of transformerless and isolated high-frequency transformer topologies show the overall advantages of the Zsource converter. Similarly, the

prototype of a 3.3kW solar-powered electric car charger based on an improved insulation Z Source inverter is proposed. However, the Zsource topology cannot be modularly expanded to obtain higher power; passive components make the impedance network and photovoltaic port generate high ripple and reduce efficient maximum power point tracking (MPPT).

## B. Contributions

This journal introduces the development of integrated, modular, and V2G-supported high power density power converters for electric vehicles that are charged from photovoltaic panels and the AC grid. Figure 1 shows the three-port block diagram of a solar-powered electric vehicle charging converter with a central DC link. There are three sub-converters inside: one unidirectional DCVDC converter for photovoltaics, bidirectional DCVAC inverters connected to the AC grid, and isolated bidirectional inverters DCVDC converter for electric vehicles. DC charging for electric vehicles is implemented here, unlike Chademo and the Combined Charging Standard (CCS) promotes smart charging, fast charging and V2G. Smart charging allows electric vehicle charging to follow photovoltaic power generation, energy prices and regulatory prices. The developed three-port architecture has three advantages. First, since EV and PV are essentially CC, the internal DCLink is used to exchange power between the three sub-drives. Second, the grid-connected inverter is essentially two-way, because it needs to feed photovoltaic energy into the grid and extract the charging energy of electric vehicles from the grid. So, the isolated DCVDC converter used in the EV is also bidirectional, enabling V2G operation. Third, a single DC V AC inverter is sufficient to connect PV and EV to the grid. This makes the converter cheaper and smaller. Generally, if the built-in converter is not used, two inverters are required, one for PV and one for EV.

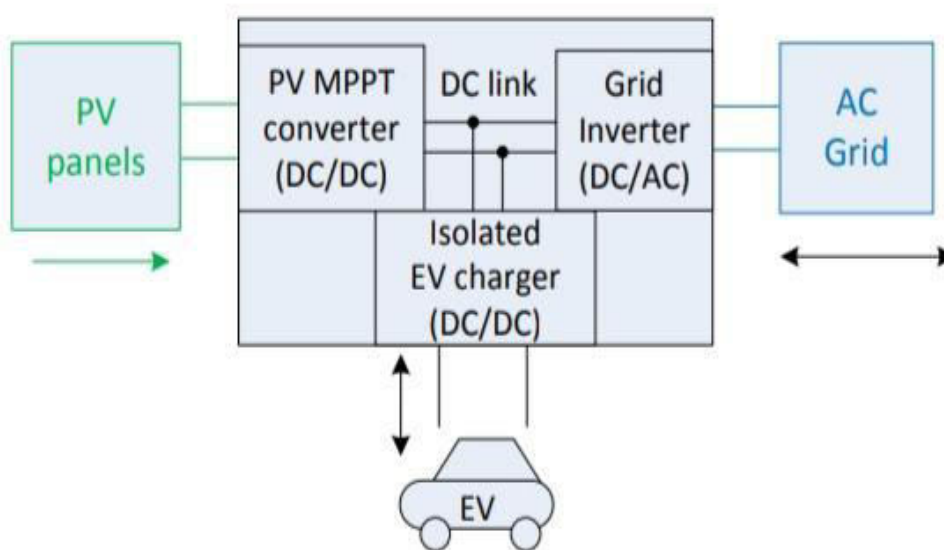


Fig. 1 – Block diagram of the grid connected bidirectional 10kW three-port EV-PV charger

The key aspects of the converter design are to achieve high efficiency, high power density, modularity and low power consumption cost. Compared with previous works, the contribution of this work is,

- Develop high-power, bi-directional, isolated, three-port power converters for direct DC charging of electric vehicles, photovoltaic and AC networks. It can be seen from the literature review that such a converter does not currently exist.
- The combined use of SiC devices, high switching frequency, interleaving and KoolM inductors leads to the developed converter having higher partial and peak load efficiency and three times the power density compared to existing solutions.



- Design a closed-loop control and use converters to achieve four different energy flows PV EV, PV Grid, Grid EV and EV Grid (that is, V2G).
- The developed converter is constructed in a modular manner and can be used as a DC V2G EV charger or as a DC V2G electric car charger. In addition, multiple DC V2G EV charger modules can run in parallel to expand the power range from 10 kW to 100 kW and is used for fast charging of electric vehicles. This will not happen with the next generation of solar-powered electric car chargers.
- The converter is designed to be compatible with IEC, Chademo and CCSV/Combo DC charging standards. Regarding ripple, harmonics, voltage range and insulation requirements, it has been tested for load VV2G operation using Nissan Leaf EV. Solar chargers currently developed for electric vehicles do not meet the standards for these commercial uses.

### C. Paper Organisation

Section 3 describes the EVPV power converter specifications and EV charging requirements standard. Sections 4, 5 and 6 provide detailed design procedures and loss models of isolated DC V DC converters for photovoltaic, bidirectional DC V AC inverter connected to the grid and DC V DC converter for charging electric vehicles. In section 7 closed-loop control of each of the three sub-converters is introduced. Section 8 describes the experimental prototype that developed and measured the waveform and efficiency of the three-port converter.

### DC/AC Grid Inverter:

The DCVAC stage uses a standard three-phase inverter with three branches and six switches, and the operating voltage is 750V DC link. This converter uses sinusoidal PWM with FSW = 47kHz. The inverter is designed for both purposes as It draws and feeds up to 16A of current to the network. As the converter adopts a hard switching operation, SiC C2M0025120D uses MOSFETs with lower  $R_{ds(on)}$  and their body diodes. The gate resistance is  $15.1\Omega$  for turn-on and  $5.1\Omega$  for turn off. At the inverter input, six 470 $\mu$ F electrolytic capacitors, connected two in series form the DC-link. Three LCL filter, one per phase are used at the inverter output for filtering out the harmonics as shown in Fig. 3[41], [42]. It's composed of  $L_{abc} = 236\mu$ H (E65 40 $\mu$  KoolM $\mu$ , N=32,  $RL=11$ m $\Omega$ );  $L_{fab} = 140\mu$ H (E42 N87, N=36,  $RL=21$ m $\Omega$ ) and a capacitor  $C_{f1}=8\mu$ F. Detailed control using sinusoidal PWM and loss modelling of the three phase inverter are well studied in literature and hence not presented again in this paper. The estimated converter efficiency including the losses in the switches, filters and control circuitry (based on section III.D) is shown in Fig. 6(c) with a peak value of 98.05%.

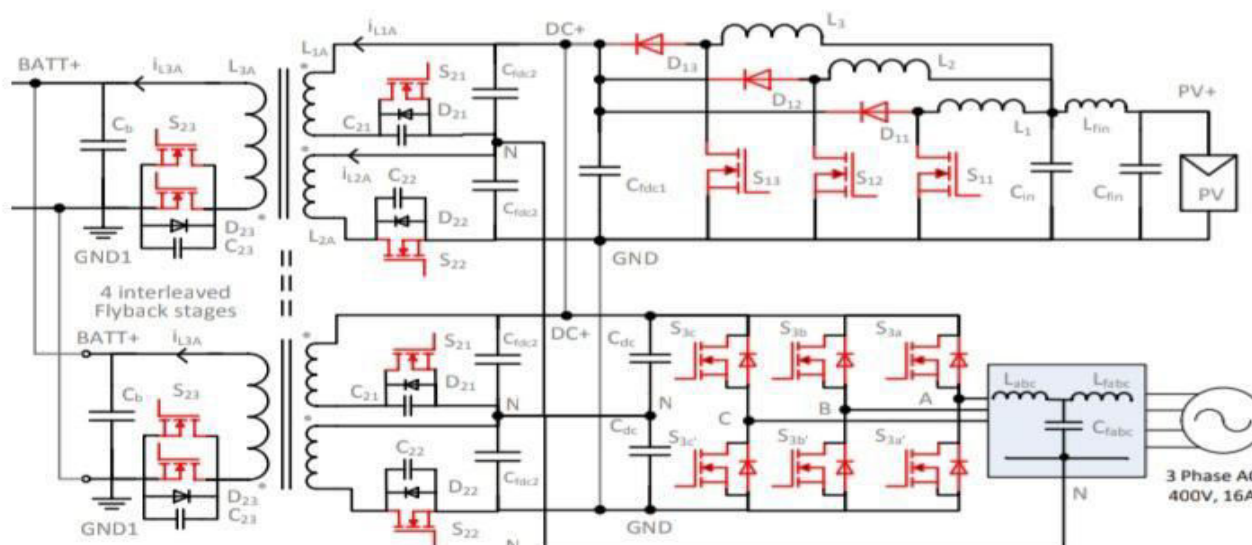


Fig. 3 – Topology of the three port EV-PV converter with a central DC-link

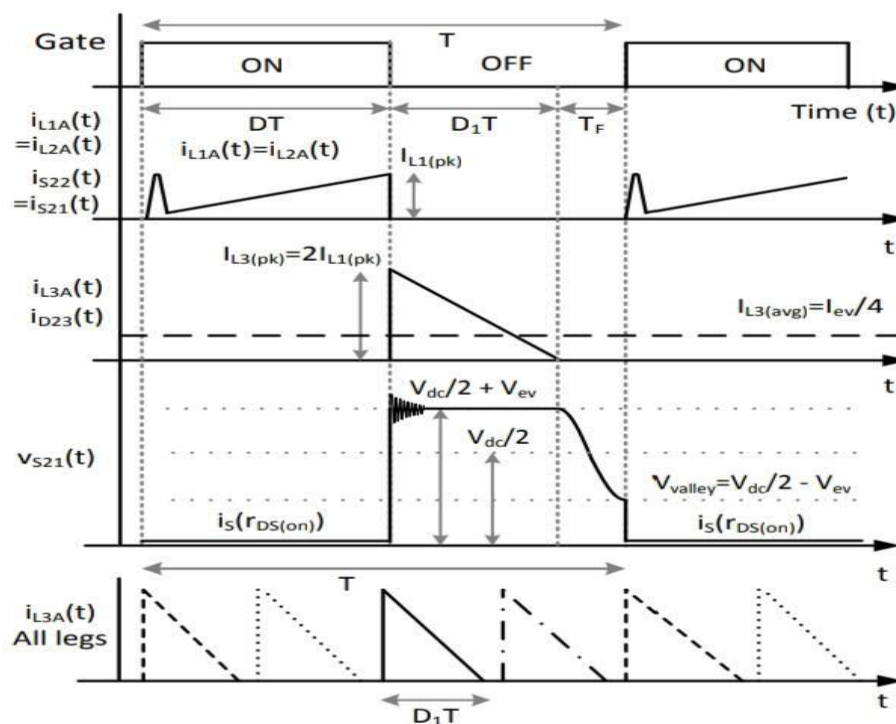
## II. ISOLATED BIDIRECTIONAL DC/DC CONVERTER FOR EV

EV's isolated bidirectional DC V DC converter consists of four interleaved flyback converters (Figure 3). MOSFETs and antiparallel diodes are used on both sides of the transformer for bi-directional operation. Every 2.5 kW flyback module has three winding transformers (turns ratio is 1: 1: 1) and there are two windings in series on the DC link. Figure 3 shows the third winding on the secondary (primary) side and the EV battery (secondary) side. For  $I_{ev}=30A$ , the corresponding output secondary current in each 2.5kW unit is  $I_{ev(m)}=7.5A$ . This difference in the primary and secondary voltages generate high secondary currents (up to 30 A). Therefore, the two MOSFETs are Parallel on the secondary side to reduce conduction losses. Flyback uses diodes C4D15120A and C2M0080120D MOSFET with  $20\Omega$  on and off gate resistors. There are two main reasons for choosing a flyback for EV converters. First, the topology provides isolation as electric vehicle charging standard requirements. Second, the flyback implemented here can be operated in both directions. There are only four switches (two on the DCLink side and two in parallel on the EV side). For other topologies, such as a dual for active bridge or resonant converter, we need 8 switches (or more in parallel to get higher current).

### A. Operation Of Interleaved Bidirectional Flyback In Quasi-resonance

The flyback converter operates in quasi-resonant (QR) mode for load and V2G operation, which has the following features:

- It can achieve MOSFET valley switching, thereby reducing conduction loss at zero voltage (ZVS) or low voltage switching (LVS).
- Resonant capacitors (C21, C22, C23) absorb and quench energy, so the loss due to disconnection is almost zero.
- Noise (DV / DT) during the shutdown is reduced by a resonance condenser.
- The quasi-resonant operation is on the border between DCM and CCM and has a lower effective value.



The waveform of the quasi-resonant operation of an IBFC with two primary and one secondary winding (from top to bottom) is S21 switch door signal; current through inductors L1A, L2A and switches S21 and S22; current through inductor L3A and switch S23, the drain-source voltage  $V_{s21}$  through switch S21; the net output current of the four interleaved IBFCs.

When the secondary diodes are conducting, the voltage across the switch is the sum of the input voltage,  $V_{dc}/2$  and the reflected secondary voltage,  $V_{RO}$ . Based on Table I,  $V_{RO}=V_{ev}$  and ranges from 50-500V. The maximum MOSFET drain-source voltage  $V_{ds(max)}$  is:  $V_{ds(max)}=V_{dc}/2+V_{RO(max)}+V_{trans}=375+500+V_{trans}\leq 1200V$  (22) where  $V_{trans}$  is the turn-off voltage transient due to the leakage inductance of the transformer (Fig. 7). Split windings are hence used on the primary side to ensure that  $V_{ds(max)}<1200V$  ( $D+D1$ )  $T<t<T$ : As soon as the diode current reaches zero, the resonant capacitors C21, C22 begin to exchange energy with the primary inductors. This causes an LC oscillation on the MOSFET drain-source voltage with a period of  $(2TF)$ , as shown in Fig. 7. The MOSFET is hence turned ON at the bottom of the valley when the voltage is at its lowest to reduce the turn-on losses:  $V_{ds(min)}=V_{valley}=V_{dc}/2-V_{ev}$  (23)  $TF=\pi\sqrt{L1AC_{ds(net)}}$  (24)  $C_{ds(net)}=C21+C_{ds,S}+C_{DD}+C_{xmer}$  (25) where  $C_{ds(net)}$  is the net drain-source capacitance due to the QR capacitor C21, C22 and due to the parasitic capacitance of the MOSFET  $C_{ds,S}$ , schottky diode  $C_{DD}$  and the transformer windings  $C_{xmer}$ . Depending on the difference  $(V_{dc}/2-V_{ev})$ , valley switching results in either ZVS or LVS at turn-on. Therefore, the net switching losses are dramatically reduced and can be zero for LVS and ZVS, respectively. This is the primary benefit of the QR operation. The sizing of the resonant capacitor must be such that it is large enough to store the maximum turn-off energy of the MOSFET considering all the operating points. From the above equations, the duty cycle  $D$ , and frequency  $f_{sw}$  for this flyback can be calculated as:  $D=2(V_{dc}/2)\sqrt{P_{ev}L1A}/f_{sw}2$  (26)  $f_{sw}=1/TF(1-D-(V_{dc}/2)V_{batt}D)$  (27) Hence, to increase the EV charging power, a larger duty cycle, a higher inductor peak current, and lower switching frequency are required, as shown in Fig. 8(a). The operating of the flyback in V2G mode is similar to the charge mode described above. The difference being that in the V2G mode, the two switches S23 are turned ON first and the diodes D21 and D22 conduct during the OFF period of the switch. Since there are four modules operating interleaved, the gate signals are phase shifted by  $90^\circ$ . The net output current,  $I_{ev}$  is the sum of the output current  $I_{ev(m)}$  of each of the four interleaved modules, as shown in Fig. 7. Table III shows the operating regions of the MOSFET for ZVS and LVS for the charge (CH) and V2G modes.  $V_{ev}$  ranges from 50-500V and is less than  $(V_{dc}/2)=375V$  for the majority of the operating range. Hence, the converter operates in ZVS for a large part of V2G mode and in LVS for a large part of charge mode.

### III. CONCLUSION

This article describes the development of a 10 kW three-port bidirectional converter for direct DC charging of electric vehicles. The developed converter is compatible with CCS and Chademo EV charging standards and can be compatible with photovoltaic arrays with a wide voltage and power range. Interleaving of converters, silicon carbide (SiC) devices and powder alloy core inductors are widely used to increase the switching frequency and keep the converter loss at a limit. This helps to triple the power density compared to traditional designs and reduces the voltage ripple on the EV and PV ports. The converter adopts a modular design, and three sub-converters are connected in the central 750 V DC link: staggered boost converters for photovoltaics, three-phase inverters for AC grids, and interleaved flyback converters for electric vehicles. Even though traditionally thought that the flyback is only suitable for low power, this article shows how to use SiC devices in QR. The flyback mode converter can achieve high efficiency even at high power. I tested three sub-converters that support four trends: PVEV, EV grid, grid and PV grid. A 10 kW prototype was built and tested, and its maximum efficiency was 95.2% for PVE, 95.4% for GridEV, and 95.4% for GridEV. PV grid is 96.4%. The developed prototype has higher peak efficiency, higher partial load efficiency and the power density is three times that of existing solutions based on AC power exchange.

### REFERENCES

- [1] C. E. Weitzel, J. W. Palmour, C. H. Carter, K. Moore, K.K. Nordquist, S. Allen, C. Thero, and M. Bhatnagar, "Silicon carbide high-power devices," IEEE Trans. Electron Devices, vol. 43, no. 10, pp. 1732–1741, 1996.
- [2] G. R. Chandra Mouli, M. Kefayati, R. Baldick, and P. Bauer, "Integrated PV Charging of EV Fleet Based on Dynamic Prices, V2G and Offer of Reserves," IEEE Trans. Smart Grids, Accept. Publ., 2017.
- [3] D. van der Meer, G. R. Chandra Mouli, G. Morales-Espana, L. Ramirez Elizondo, and P. Bauer, "Energy Management System with PV Power Forecast to Optimally Charge EVs at the Workplace," IEEE Trans. Ind. Informatics, vol. 14, no. 1, pp. 311–320, 2018.



- [4] S. A. Singh, G. Carli, N. A. Azeez, and S. S. Williamson, "Modeling, Design, Control, and Implementation of a Modified Z-Source Integrated PV/Grid/EV DC Charger/Inverter," IEEE Trans. Ind. Electron., vol. 65, no. 6, pp. 5213–5220, Jun. 2018.
- [5] G. Waltrich, J. L. Duarte, and M. A. M. Hendrix, "Multiport converter for fast charging of electrical vehicle battery: Focus on DC/AC converter," in IECON 2011 -37th Annual Conference of the IEEE Industrial Electronics Society, 2011, pp. 3626–3633.
- [6] J. Reinert, A. Brockmeyer, and R. W. A. A. De Doncker, "Calculation of losses in ferro-and ferrimagnetic materials based on the modified Steinmetz equation," IEEE Trans. Ind. Appl., vol. 37, no. 4, pp. 1055–1061, 2001.
- [7] D. H. Kim, G. Y. Cheo, and B. K. Lee, "Design and control of an optimized battery charger for an xEV based on photovoltaic power systems," J. Electr. Eng. Technol., vol. 9, no. 5, pp. 1602–1613, 2014.
- [8] C. Hamilton, G. Gamboa, J. Elmes, R. Kerley, A. Arias, M. Pepper, J. Shen, and I. Batareseh, "System architecture of a modular direct-DC PV charging station for plug-in electric vehicles," in IECON 2010 -36th Annual Conference on IEEE Industrial Electronics Society, 2010, pp. 2516–2520.





**Impact Factor:  
7.569**



# INTERNATIONAL JOURNAL OF INNOVATIVE RESEARCH

IN SCIENCE | ENGINEERING | TECHNOLOGY

 **9940 572 462**  **6381 907 438**  **ijirset@gmail.com**



[www.ijirset.com](http://www.ijirset.com)

Scan to save the contact details